*International Journal on Recent and Innovation Trends in Computing and Communication*
*ISSN: 2321-8169 Volume: 11 Issue: 9s*
*DOI: https://doi.org/10.17762/ijritcc.v11i9s.7473*
***Article Received**: 26 May 2023 **Revised:** 20 July 2023 **Accepted:** 05 August 2023*

# LFM based Wideband DOA Estimation using Deep Neural Network at Low SNR

**Nagaraju L*, Lokesh Dharma Theja ch, Puli Kishore Kumar**
Department of Electronics and Communication Engineering,
National Institute of Technology Andhra Pradesh,
Tadepalligudem-534101, India
e-mail: *nagaraju.sclr@nitandhra.ac.in, lokesh.sclr@nitandhra.ac.in, pulikishork@nitandhra.ac.in

**Abstract**— This work focuses on deep learning-based wideband direction-of-arrival (DoA) estimation for a wideband in particular LFM in case of extreme noise. We propose a convolutional neural network (CNN) that utilizes the correlation matrix to estimate and trained using multi-channel data in low SNR conditions. By using a systematic approach and treating the problem as a way to identify multiple possible DoAs, the CNN is trained to predict DoAs under different SNR conditions. This allows the CNN to accurately estimate the directions from which signals are coming, regardless of the level of noise in the environment. The architecture proposed exhibits robustness to noise, works effectively with a small number of snapshots, and achieves high resolution in angle estimation. Experimental findings demonstrate notable enhancements in performance under low SNR conditions when compared to existing methods, without the need for parameter tuning for correlated and uncorrelated sources. The enhanced robustness of our solution has broad applications in various fields, including wireless array sensors, acoustic microphones, and sonars.

**Keywords**- Deep Neural Network; DOA Estimation; LFM; Low SNR; Wideband location vector.

## I. INTRODUCTION

DoA estimation has attracted considerable attention and interest from researchers over an extended period, owing to its wide range of applications in many fields like radar, wireless and etc [1]. Localization stands out as a significant application. The estimation of angular directions can be achieved by utilizing multiple sensors arranged in specific geometric configurations, such as linear, rectangular, or circular arrays. Leveraging the observations from these sensor arrays efficiently allows for estimating the DoA of multiple sources, based on the number of antenna elements available. There are generally two main categories of DoA estimation techniques: the over-determined case, when there are fewer sources than array sensors, and the under-determined case, when the number of sources is greater than the number of array sensors [2]. This work focuses on investigating the first category, specifically addressing estimating the DoA of signals in challenging low SNR conditions has been a focus of research. MUSIC is an early technique that emerged in the field of DoA estimation is one of the initial approaches proposed for this task. And it has been followed by several variant techniques. These methods belong to the subspace category, which aims to separate the noise and signal subspaces in order to estimate the angles.

The MUSIC method utilizes pseudo-spectra computed over a predefined grid, where peaks in the pseudo-spectra correspond to estimated angles. These high-resolution subspace-based methods are also used for DOA estimation in case of wideband signals and popularly known as time-frequency MUSIC (TF-MUSIC) [3]. TF Root-MUSIC [4] introduced a significant advancement by estimating DoA from the solutions of polynomials. These techniques that rely on covariance analysis necessitate a substantial number of snapshots to accurately estimate the DoA in low SNR conditions to achieve accurate DoA estimation. Additionally, they often assume prior knowledge of the number of sources, which may not be available in practical applications. In recent years, Compressed Sensing (CS) techniques have emerged as a promising approach for DoA estimation [5]. These methods leverage the sparsity of signal sources in the spatial domain. CS methodologies can be categorized into different types as: grid-less, off-grid, and on-grid methods [6], [7] Grid-less methods achieve superior performance but come with high computational complexity [8]. To estimate DoAs, CS methods typically solve sparse minimization problems using greedy methods. An effective approach in this field is the ℓ2,1-SVD algorithm, which utilizes signal data reduction techniques along with solving the ℓ2,1-norm minimization problem in a reduced dimension. This strategy offers notable benefits such as reduced computational complexity and improved efficiency. This method was proposed in [9] and later used in [10]. However, a common drawback of these approaches is the requirement of parameter tuning, dependent on factors such as the number of snapshots and the SNR, to ensure optimal performance. Deep Learning (DL) has emerged as a recent approach for DoA estimation [11], [12]. DL methods offer advantages over optimization-based techniques: a) they require no optimization after network training, simplifying the solution to simple operations; b) parameter tuning is not necessary as in optimization-based methods,

*International Journal on Recent and Innovation Trends in Computing and Communication*
*ISSN: 2321-8169 Volume: 11 Issue: 9s*
*DOI: https://doi.org/10.17762/ijritcc.v11i9s.7473*
***Article Received**: 26 May 2023 **Revised:** 20 July 2023 **Accepted:** 05 August 2023*

reducing dependency on parameter settings; c) DL methods demonstrate resilience to data imperfections, performing well with fewer snapshots and in low SNR. Previous studies have explored DL for DoA estimation. Some focused on DoA classification using fully connected layers with signal covariance matrices [13], while others addressed channel estimation in massive MIMO systems [14]. Another approach employed a multilayer autoencoder with parallel multilayer classifiers for robustness to array imperfections [15]. However, these methods had limitations in high SNR scenarios or were restricted to two sources. Different DL architectures have been proposed, such as CNNs for DoA estimation [16] and CNNs for speech processing. Our study specifically focuses on wide-band DoA estimation, distinguishing it from previous works. In the context of acoustics, DL methods have been proposed for beamforming using sample covariance matrices [17]. However, these approaches are limited in low SNR scenarios where more sensors and snapshots are required. This work aims to address the gap in DoA estimation literature by focusing on low SNR scenarios and utilizing DL techniques. Existing methods often struggle with DoA estimation in low SNR due to deviations of the Sample Covariance Matrix estimates from the actual manifold matrix. To overcome these challenges, we propose the following contributions:

- We introduce a new method for estimating the directions of wideband signals. We develop effective training techniques for our network, demonstrating its ability to accurately predict directions even in challenging low SNR conditions, including high SNR situations.
- In this study, we introduce a deep CNN that is trained on multi-channel data. This data is obtained from the complex-valued covariance matrix, which includes real, imaginary, and phase components as separate channels.
- Here we use 2-D convolutional layers in the CNN to accurately predict the angle of the source, improving the estimation of direction in situations with low SNR.
- We use a method that divides the desired angular region into discrete values (on-grid), treating the task of estimating directions as a classification problem with multiple possible labels.

The results demonstrate that the proposed CNN surpasses competing methods in low SNR DoA estimation. It exhibits resilience in estimation, even with a small number of snapshots and varying angular separations of the sources. Moreover, the CNN shows enhanced robustness in the presence of SNR mismatches and achieves accurate inference of both the number of incoming sources and their corresponding DoAs with minimal errors and high confidence levels.

## II. DATA MODEL

### A. *Linear Frequency Modulating Signal*

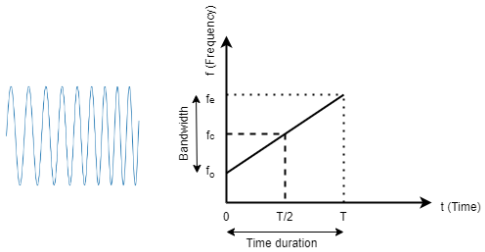


Figure 1. LFM signal

We know that, we have the following equation for wave,

$$s(t) = a\,cos\big(2\pi(ft + \emptyset)\big) \quad (1)$$

to generate a linear frequency modulating (LFM) signal, we need to increase the frequency of the carrier signal with time. Let the frequency of the transmitted signal be a linearly increasing function of time as shown in the figure 1. The equation of the linearly increasing line shown in figure 1 with slope $\mu_o$ = B/T, (where B is bandwidth and T is the time duration of the signal) and y-intercept $f_o$ is

$$f = \mu_0 t + f_0 \quad (2)$$

substituting equation 2 in equation 1

$$s(t) = a\,cos\big(2\pi((\mu_0 t + f_0)t + \emptyset)\big) \quad (3)$$

$$s(t) = a\,e^{\left(j2\pi((2f_0 t + \mu_0 t^2) + \emptyset)\right)} \quad (4)$$

In general, [18] the LFM signal is represented as equation 5, is a matter of convention and mathematical convenience (see appendix A).

$$s(t) = a\,e^{\left(j\pi((2f_0 t + \mu_0 t^2) + j\emptyset)\right)} \quad (5)$$

where $a$ is the signal amplitude, $f_o$ is the initial frequency, t is time vector, $\mu_o$ is the chirp or sweep rate and φ is the initial phase offset of the signal.

### B. *Signal Model*

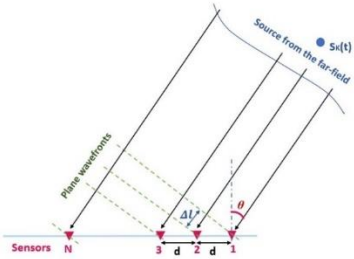


Figure 2. Signal model

Let us consider an N-element uniform linear array (ULA) with inter element spacing as d = λ/2 , where λ is wavelength of the incoming signals λ = c/f (f is highest frequency of incoming signals in case of multi-source) and K uncorrelated wideband sources from far-field are impinging on the antenna array as shown in the figure 2. Then [18] the received signal from antenna array is modeled as

*International Journal on Recent and Innovation Trends in Computing and Communication*
*ISSN: 2321-8169 Volume: 11 Issue: 9s*
*DOI: https://doi.org/10.17762/ijritcc.v11i9s.7473*
***Article Received**: 26 May 2023 **Revised:** 20 July 2023 **Accepted:** 05 August 2023*

$$x(t) = \sum_{i=1}^{M} \boldsymbol{a}\,(v,t)\; s_i(t) \;+\; \boldsymbol{n}(t) \qquad (6)$$

In the wideband model we have time-varying location vector $\boldsymbol{a}(v,t)$ of the array, whereas in the distributed narrowband model, it remains constant. The random variable $s_i(t)$ represents the temporal characteristics of the wideband source, **n**(t) represents additive zero-mean white noise vector.

One way to address this challenge is by employing a time-varying location vector to capture the dynamic nature of the wideband signal. This location vector includes not only the central angle of the source but also the width that represents the angular spread of the signal. By incorporating the time-varying location vector, we can effectively model the wideband signal and apply techniques like coherent wideband beamforming for accurate source localization. On the other hand, the FRFT-based beamforming approach assumes a time-invariant location vector in the Dechirping domain. In this specialized domain, the FRFT is utilized to steer the array response towards a specific direction. By assuming a time-invariant lo cation vector, we can leverage the FRFT for source localization without the need to account for temporal variations in the location vector [18].
signal received by the reference antenna element in the array is without delay and represented as equation 5, signal received at the $k^{th}$ antenna element with respect to reference antenna element is time delayed by $\tau_k = (k-1)d\sin(\theta)/c$, where k = 1,2,...,N, θ is the incident angle of the wideband source and c is the speed of the light.

$$x_k = a\, e^{\{j2\pi(2f_0(t-\tau_k)+\mu_0(t-\tau_k)^2\}+j\emptyset} \qquad (7)$$

$$= a e^{j\pi(2f_0 t+\mu_0 t^2)+j\emptyset}\, e^{j\pi(-2f_0\tau_k+\mu_0{\tau_k}^2-2\mu_0 t\tau_k)} \qquad (8)$$

Therefore, the equation 8 as two terms, first term is the LFM signal transmitted i.e., source signal and the second term is time varying location vector. As discussed earlier this time-varying location vector can be converted into time-invariant form by using tools like FRFT. Which will result in array steering matrix as

$$\boldsymbol{A}(\theta) = e^{j\pi(-2f_0\tau_k+\mu_0{\tau_k}^2)} \qquad (9)$$

since the τk is depending on the antenna elements and incident angles, $\boldsymbol{A}(\theta) \in C^{N\times M}$. And the distance between antenna elements is very small so, $\mu_0{\tau_k}^2$ term can be neglected [19].

$$\boldsymbol{A}(\theta) \approx e^{j\pi(-2f_0\tau_k)} \qquad (10)$$

$$\boldsymbol{A}(\theta) \approx [\boldsymbol{a_1}(\boldsymbol{\theta})\boldsymbol{a_2}(\boldsymbol{\theta})\boldsymbol{a_3}(\boldsymbol{\theta})\ldots\boldsymbol{a_M}(\boldsymbol{\theta})] \qquad (11)$$

$$\boldsymbol{a_i}(\theta) \approx [\mathbf{1} \quad e^{-j\pi\, 2f_0 sin(\theta)/c} \quad e^{-j\pi\, 4f_0 sin(\theta)/c}\ldots \quad .e^{-j\pi\, 2f_0\,(N-1)sin(\theta)/c}\,]^{\mathrm{T}} \qquad (12)$$

where i = 1, 2,...,M and θ ∈ [−90° 90°]. The received signal is constructed as

$$\boldsymbol{x(t)} = \boldsymbol{A}(\theta)\boldsymbol{s}(t) + \boldsymbol{n}(t) \qquad (13)$$

The received signal correlation vector is

$$\boldsymbol{R}_x = E\,[x(t).x^H(t)] = \boldsymbol{A}(\theta)\boldsymbol{R}_s\boldsymbol{A}^H(\theta) + \sigma_e^2\boldsymbol{I}_N \qquad (14)$$

where $\mathbf{R}_s$ represents diagonal source correlation matrix E[**s**(t) $\mathbf{s}^H$(t)]. In practice the received signal correlation vector is obtained as

$$\widetilde{\boldsymbol{R}}_{\boldsymbol{x}} = \frac{\mathbf{1}}{\boldsymbol{T}}\sum_{t=1}^{T}\boldsymbol{x}(t).\boldsymbol{x}^H(t) \qquad (15)$$

## III. PROPOSED DEEP NETWORK METHOD FOR DOA

In this section, we present our approach to DoA estimation, which involves formulating it as a multilabel classification task. We provide details on how we manage the data and label it in Section 3.1. Additionally, in Section 3.2, we de scribe the architecture of the CNN that we employ to predict the DoAs. The CNN utilizes convolution layers to extract relevant features from the multi-channel in put data. These extracted features are then processed by the fully connected (FC) layers to estimate the DoAs based on a grid that has been pre-selected.

### *A. Data Handling and Annotation*

To model DoA prediction, we treat the task as a classification problem where each data sample can be associated with multiple labels or categories simultaneously. We define a grid G consisting of 2G+1 discrete points with a resolution ρ, covering the range from $-\varphi_{max}$ to $\varphi_{max}$ in increments of ρ degrees. The covariance matrix is calculated for K randomly selected angles from the grid G at each SNR level, according to equation 14.

The input data for our CNN is represented by a real-valued N×N×3 matrix, where the third dimension corresponds to different channels.

Table 1. Input data to CNN.

| S. No | Channel | Input |
|---|---|---|
| 1 | First | $Re\{\mathbf{R_x}\}$ |
| 2 | Second | $Im\{\mathbf{R_x}\}$ |
| 3 | Third | $\angle\{\mathbf{R_x}\}$ |

Based on the well-known universal approximation theorem [20], it is proven that a specific type of neural network architecture, which includes a single hidden layer and a multilayer perceptron, has the capability to approximate continuous functions within a bounded region in $R^n$. In the context of our specific task, which involves multilabel classification, our main objective is to develop a ma chine learning model, represented as function f, that can effectively map input data from the space $R^{N\times N\times 3}$ to the desired output space Z. During the training phase, the network is trained using the true covariance matrix. However, for testing and evaluation purposes, we utilize the sample covariance described in equation 15 since the true covariance matrix is not available. This guarantees that during the evaluation phase, all input samples are considered as 'new' or 'un known' data with respect to the training procedure.

*International Journal on Recent and Innovation Trends in Computing and Communication*
*ISSN: 2321-8169 Volume: 11 Issue: 9s*
*DOI: https://doi.org/10.17762/ijritcc.v11i9s.7473*
***Article Received**: 26 May 2023 **Revised:** 20 July 2023 **Accepted:** 05 August 2023*

### *B. Architecture of Proposed CNN*

The proposed CNN architecture draws inspiration from established convolutional structures commonly employed in image processing literature [21], [22]. However, necessary modifications have been introduced to address the specific requirements and characteristics of our problem. The visualization of the CNN architecture is as shown in figure 3.

The function f, which has adjustable parameters, is realized using a CNN architecture comprising 8 layers.

$$f(\boldsymbol{X}) = f_8(f_7(\ldots(f_1(\boldsymbol{X}))) = z \quad (16)$$

The function {fi(.)} i = 1,2,3,4 represents a sequence of convolutional layers, the basic information of the architecture is tabulated in table 2. After the activation layer following f4(.), a reshaping layer is used to convert the tensor output into a vector size M × M. In the first layer, the convolution operation is performed on the input data X and the kernel K, both of which have specific dimensions as RN×N×3 and Rk×k×3 respectively, which is given as:

$$(\boldsymbol{X} * \boldsymbol{K})_{m,n} = \sum_{i=1}^{k}\sum_{j=1}^{k}\sum_{k=1}^{3} K_{i,j,k} X_{\delta(m-1)+i,\delta(n-1)+j.k} \quad (17)$$

The mathematical operation performed on the qth filter at the ℓth convolutional layer is performed for values of m and n ranging from 1 to M, where M is calculated as $\lfloor (N - k)/\delta \rfloor + 1$. In this operation, the parameters involved are as follows: Input: We have X[ℓ−1], an M[ℓ−1] ×M[ℓ−1] ×$n_C^{[\ell-1]}$ matrix. In this case, X [0] = X and M [0] = N, with $n_C^{[0]}$ = 3. Filter: The kernel is denoted as $\mathbf{K}_q^{[\ell]}$ dimensions k[ℓ] × k[ℓ] × $n_q^{[\ell-1]}$. Stride: The stride is δ[ℓ]. Bias: The bias term is $b_q^{[\ell]}$. Output: The resulting output is $\mathbf{X}_q^{[\ell]}$, an M[ℓ]×M[ℓ] matrix. The convolution operation can be explained as follows:

To compute the value of $(\mathbf{X}^{[\ell-1]} \times \mathbf{K}_q^{[\ell]})_{m,n}$, we sum the products of $\mathbf{K}_{i,j,k}^{q,[\ell]}$ and $\mathbf{X}_{\delta(m-1)+i,\delta(n-1)+j,k}^{[\ell-1]}$ for i = 1...k[ℓ], j = 1...k[ℓ], and k = 1... $n_C^{[\ell-1]}$ . We then add the bias term $b_q^{[\ell]}$.

In simpler terms, the output matrix $\mathbf{X}_q^{[\ell]}$ is obtained by sliding the filter $\mathbf{K}_q^{[\ell]}$ over the input matrix $\mathbf{X}^{[\ell-1]}$ with a stride of $\delta^{[\ell]}$. At each position, the corresponding elements of the filter and input are multiplied and summed, along with the bias term. This process is repeated for each position in the output matrix, resulting in the final M[ℓ] × M[ℓ] matrix.

Table 2 The table represents the basic architecture information.

| Layer | Description | Filters | Kernel Size | Stride ($\delta$) |
|---|---|---|---|---|
| $f_1(.)$ | 2D-Convolutional layer<br>Batch normalization<br>ReLU | 256 | 3 × 3 | 2 |
| $f_2(.)$ | 2D-Convolutional layer<br>Batch normalization<br>ReLU | 256 | 2 × 2 | 1 |
| $f_3(.)$ | 2D-Convolutional layer<br>Batch normalization<br>ReLU | 256 | 2 × 2 | 1 |
| $f_4(.)$ | 2D-Convolutional layer<br>Batch normalization | 256 | 2 × 2 | 1 |

## IV. CNN LEARNING PROCESS

To train the proposed CNN, we utilized a grid resolution of ρ = 1° and narrow grid (G = 60). We used $\varphi_{max}$ = 60°, resulting in a narrow grid set $G_n$ ={−60°,...,60°} with 121 grid points. The CNN's output dimension, after binary transformation of the DoAs, is 121. Consequently, the training process for the proposed network was conducted independently for each network. To reduce the required training data and enable DoA prediction for various snapshots of the Sample Covariance Matrix estimate, we employed data from the true co variance matrix. One benefit of our method is that the CNN has the capability to learn the number of sources by treating it as a task of classifying multiple classes. Therefore, we employed training approach with a Known Source Count. This approach assumes a known number of sources and is suitable when the number of sources is predetermined. 4.1. Training Approach with a Known Source Count Here we outline the process of generating synthetic data when the number of sources is known in advance. For the case of K=1 sources, we generate pairs of DoA angles from all possible combinations within the angular grid G, resulting in 2G+1 K angle pairs. For each SNR value, we generate the input data X by utilizing the actual covariance matrix obtained from equation 15, along with the appropriate labels as explained in Section 3.1. The Dechirped signal is taken at different SNR's, especially at low SNR's ranging from-20dB to 0dB, with a step size of 5dB.

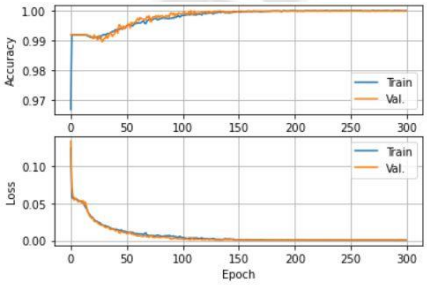


Figure 4. The performance and error metrics during the training and validation stages of the CNNare illustrated for a fixed number of sources and a narrow grid $G_n$.

Table 3 Training and Validation Metrics for CNN Accuracy and Loss.

| S.No. | Parameter | Result |
|---|---|---|
| 1. | Training Accuracy | 99.99 |
| 2. | Validation Accuracy | 99.97 |
| 3. | Training loss | $3.86 \times 10^{-4}$ |
| 4. | Validation loss | $7.18 \times 10^{-4}$ |
| 5. | number of epochs | 300 |
| 6. | Accuracy score | 100% |

*International Journal on Recent and Innovation Trends in Computing and Communication*
*ISSN: 2321-8169 Volume: 11 Issue: 9s*
*DOI: https://doi.org/10.17762/ijritcc.v11i9s.7473*
***Article Received**: 26 May 2023 **Revised:** 20 July 2023 **Accepted:** 05 August 2023*

For the narrow angular region with G=60, we generate $\binom{2G+1}{K}$ training examples per SNR. We specifically focus on low SNR scenarios for training the proposed CNN, considering SNR values of {−20,−15,−10,−5,0}dB. We noticed that training in the low SNR range, which represents challenging conditions, is effective in obtaining accurate predictions even at higher SNRs, as discussed in Section 5.2. Training multiple models per SNR would require storing many parameters, and in the testing, the exact SNR would need to be known, which is often not feasible. Therefore, we opt for joint training across the range of low SNRs to overcome these limitations and achieve robust performance. The CNN training process is conducted offline using randomly split data, with 90% allocated for training and 10% for validation. Figure 4 display the binary accuracy and loss during training and validation in each cycle for the specified numberof sources, the CNN is trained using the corresponding narrow grid. Training andvalidation metrics for CNN accuracy and loss are shown in table 3.

## V. SIMULATIONS AND DISCUSSIONS

Here comprehensive simulation results to estimate the performance of the proposed CNN in DoA estimation across different scenarios. Initially, in section 5.1 we summarize the methods for comparison, evaluating the CNN's performance under the assumption of known source count. Then we present results demonstrating the CNN's capability to predict DoAs in both on-grid and off-grid scenarios in section 5.2.

Throughout the training and testing phases of our experiments, we employ a ULA consisting of 16 antenna elements. These elements are evenly distributed at a separation distance of half-wavelength (d=λ/2).

Table 4. The trainable parameters for *G* = 60 of the CNN architecture.

| S.No. | Layer | Parameter |
|---|---|---|
| 1. | First convolutional | 7680 |
| 2. | Second convolutional | 262912 |
| 3. | Third convolutional | 262912 |
| 4. | Fourth convolutional | 262912 |
| 5. | First FC | 16781312 |
| 6. | Second FC | 8390656 |
| 7. | Third FC | 2098176 |
| 8. | Fourth FC | 124025 |

The training parameters of the CNN architecture at each stage are tabulated and shown in table 4. Overall, the CNN architecture we propose involves traininga significant number of parameters, approximately 28.2 million in total. Through-out all experiments, the SNR is defined according to the reference [23].

$$SNR = 10\ log_{10} \frac{min\{\sigma_1^2,\sigma_2^2,\dots\sigma_K^2\}}{\sigma_e^2} \quad (18)$$

Following the training process, the CNN provides predictions

$$\hat{\boldsymbol{p}} = f(\widetilde{\boldsymbol{X}}) = \begin{bmatrix} \hat{p}_1 \\ \vdots \\ \hat{p}_{2G+1} \end{bmatrix} \quad (19)$$

$\widetilde{\boldsymbol{X}}$ be a matrix of dimensions N×N×3 where X:,:,1 represents the real part of $\widetilde{\boldsymbol{R}}_y$, X:, :, 2 represents the imaginary part of $\widetilde{\boldsymbol{R}}_y$, and X:, :, 3 represents the phase.

### *A. Evaluation and Comparison with Other Approaches*

Here is the summary of the methods employed for comparison against the proposed CNN.

1. Conventional beamforming [1]
2. LFM-MUSIC [3]
3. LFM-R-MUSIC [4] The comparison includes methods commonly found in the literature of DoA estimation: methods 1 represent classical beamforming approach, method 2 rep resents subspace-based method and method 3 represents parametric based DoA estimation method. For the on-grid methods (MUSIC), we adopt a grid resolution of ρ = 1o, matching that of the CNN. Additionally, we compute CRLBs for the estimation accuracy [24], [25].

### *B. Performance comparison of proposed technique*

During testing, the CNN outputs a set of probabilities using equation 19. After determining the K number of sources, we identify K highest probabilities from the CNN's output. The indices on the grid that correspond to these probabilities are considered as the estimated DoAs. To evaluate the performance of the CNN architecture, we employ the RMSE as the statistical performance metric. The RMSE is defined as follows:

$$RMSE = \sqrt{\frac{1}{T_t K}\sum_{m=1}^{T_t}\left(\theta_k^{(m)} - \hat{\theta}_k^{(m)}\right)^2} \quad (20)$$

where for the m[th] testing example true DoA's are denoted as $[\theta_1^{(m)}, \theta_2^{(m)}, \dots \theta_k^{(m)}]^T$ while the estimated DoA's are represented as $[\theta_1^{(m)}, \theta_2^{(m)}, \dots \theta_k^{(m)}]^T$ The variable $T_t$ represents each experiments total testing samples.

In the first experiment, we examine scenarios where the SNR dB is low. The array receives a signal with an SNR of-10 dB, while the first signal's direction varies from −60o to an increasing step of 1°. We collect T=1024 snapshots to estimate the spatial covariance matrix (SCM). The trained CNN is then tested for all possible ON-GRID angles, the error obtained for all predictions is zero as shown in figure 5, the probability of detecting the signal is 99.12%. And the performance of all the angles is shown in figure 6.

Now, we assess the effectiveness of the CNN we proposed in estimating the DoA for single sources placed at an angle of θ = 15° is evaluated. To assess its performance, the RMSE is calculated based on 1000 Monte Carlo simulations at each SNR level, with the sample covariance estimated using T=1 snapshots. Figure 7 illustrates the RMSE results, along with the CRLB calculated based on [24] for each SNR. In the range of low SNR, the CNN exhibits impressive performance with

*International Journal on Recent and Innovation Trends in Computing and Communication*
*ISSN: 2321-8169 Volume: 11 Issue: 9s*
*DOI: https://doi.org/10.17762/ijritcc.v11i9s.7473*
***Article Received**: 26 May 2023 **Revised:** 20 July 2023 **Accepted:** 05 August 2023*

RMSE values comparable to the robust TF-MUSIC method. Importantly, the CNN exhibits a distinct advantage by eliminating the need for parameter tuning, which is particularly beneficial in real-world situations where the SNR is uncertain or subject to slight changes. Additionally, the findings reveal that in high-SNR conditions, the RMSE reaches a lower limit for all methods based on a predefined grid. However, it is worth noting that only the grid-less estimator R-MUSIC has the potential to approach the CRLB in terms of accuracy.

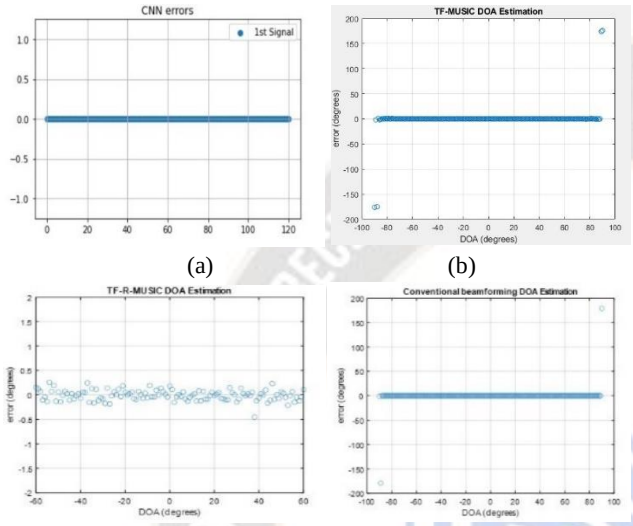


Figure 5. We evaluate and compare the accuracy of various methods for direction of arrival (DoA) estimation, including: (a) the proposed CNN, (b) TF-MUSIC, (c) TF-R-MUSIC, and (d) conventional beamforming. The results indicate that the CNN outperforms the other methods, demonstrating the errors and performance that is comparable to the conventional estimators.

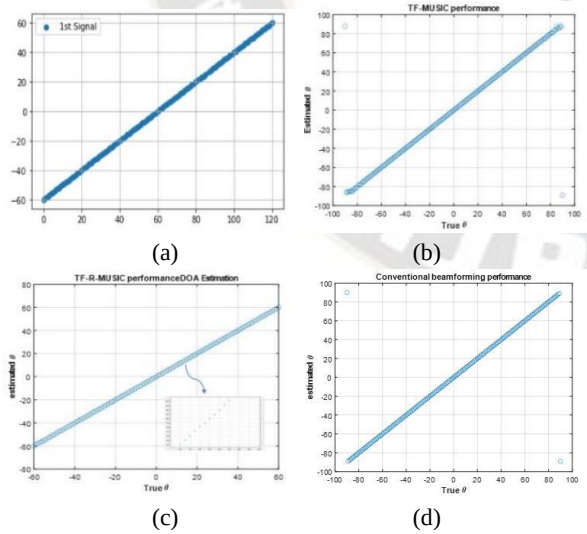


Figure 6. The DoA estimation performance for on-grid angles θ within the range of [−60º,60º] at-10 dB SNR using T=1024 snapshots. The DoA estimation results of various methods are shown for comparison, including: (a) Proposed CNN, (b) Time-Frequency-MUSIC, (c) Time-Frequency Root-MUSIC, (d) Conventional beamforming

The trained CNN is evaluated by testing it at an SNR of-10dB for various off-grid angles. Although the predictions made by the CNN are not error-free, the probability of detecting the signal accurately is 93% as shown in figure 8. This indicates that the CNN can perform well in identifying the presence of the signal, despite some errors in the predicted angles.

The performance of the trained CNN is evaluated for predicting off-grid angles within a range of −59.7º to +60.7º. The CNN is tested on these angles, and the results are plotted in a figure 9. The plot provides an overview of the CNN's performance in accurately predicting the off-grid angles across the given range.

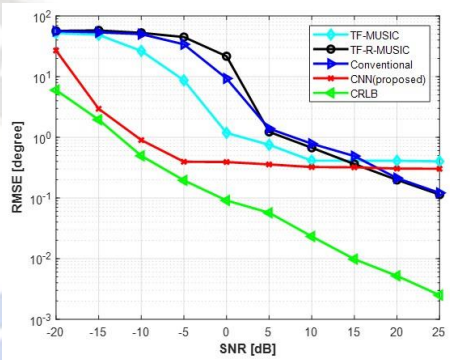


Figure 7. RMSE versus SNR for the estimation of a single source DoA using T=1 snapshot. Remarkably, in the low-SNR range, the proposed CNN exhibits superior performance compared to subspace-based methods, indicating its effectiveness in challenging conditions.

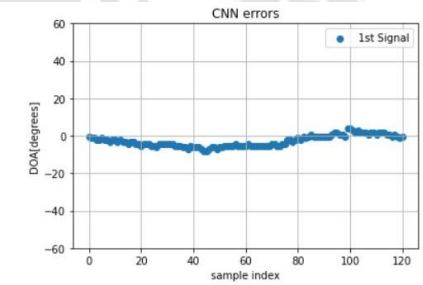


Figure 8. CNN Prediction of OFF-GRID angles

## VI. CONCLUSION

This research paper introduces an innovative method for predicting DoA in low SNR scenarios utilizing a deep CNN equipped with 2D filters. We address the challenge of angle estimation by treating it as a multi-label classification problem and employing an on-grid approach. The integration of 2-D

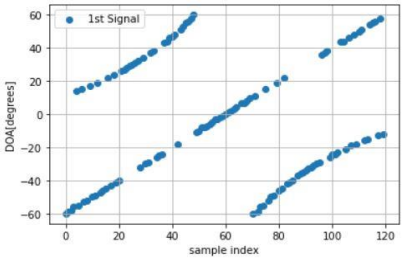


Figure 9. CNN Errors For Prediction of Different OFF-GRID Angles

*International Journal on Recent and Innovation Trends in Computing and Communication*
*ISSN: 2321-8169 Volume: 11 Issue: 9s*
*DOI: https://doi.org/10.17762/ijritcc.v11i9s.7473*
***Article Received**: 26 May 2023 **Revised:** 20 July 2023 **Accepted:** 05 August 2023*

convolutional layers in our CNN allows for efficient feature extraction from multi-channel input data, enabling effective information transfer to fully connected layers, resulting in improved DoA estimation in low SNR scenarios. Additionally, we propose a specific training strategy for a fixed number of sources, which is particularly suitable when the source number is known beforehand, a common assumption in related research. To validate our approach, we compare it in comparison to cutting-edge techniques and utilize the CRLB as a benchmark. Evaluating the performance of our CNN, we measure its RMSE for angles that are not on the grid in var ious configurations, including a wide range of SNRs and fixed directions. Our results demonstrate superior performance in low SNR conditions and highlight the CNN's potential for resolving closely spaced angles. Future work may focus on further exploring its capabilities in low SNR scenarios.

## ACKNOWLEDGMENT

The authors would like to thank SERB, DST Govt. of India for the project grant under EEQ/2019/000723. This work is sponsored under this project.

## CONFLICTS OF INTEREST

The authors have no conflicts of interest to declare.

## REFERENCES

[1] M. Mart´ınez-Ram´on, A. Gupta, J. L. Rojo-´Alvarez, C. Christodoulou, K. Cools, Machine learning applications in electromagnetics and antenna array processing [book review], IEEE Antennas and Propagation Magazine 64 (4) (2022) 178–179. doi:10.1109/MAP.2022.3178921.

[2] C.-L. Liu, P. P. Vaidyanathan, Remarks on the spatial smoothing step in coarray music, IEEE SP Letters 22 (9) (2015) 1438–1442. doi:10.1109/LSP.2015.2409153.

[3] L. Hachad, O. Cherrak, H. Ghennioui, F. Mrabti, M. Zouak, Doa es timation based on time-frequency music application to massive mimo systems, in: 2017 International Conference on Advanced Technolo gies for Signal and Image Processing (ATSIP), 2017, pp. 1–5. doi:10.1109/ATSIP.2017.807558.

[4] R. Zhagypar, K. Zhagyparova, M. T. Akhtar, spatially smoothed tf-root-music for doa estimation of coherent and non-stationary sources under noisy conditions, IEEE Access. doi:10.1109/ACCESS.2021.3095345.

[5] C. A. D. Mahdi Khosravy, Nilanjan Dey, Compressive Sensing in Health- care, Vol. 11, Mara Conner, 2020.

[6] S. Ganguly, I. Ghosh, R. Ranjan, J. Ghosh, P. K. Kumar, M. Mukhopadhyay, Compressive sensing based off-grid doa estimation using omp algorithm, in: 2019 6th International Conference on Signal Processing and Integrated Networks (SPIN), 2019, pp. 772–775. doi:10.1109/SPIN.2019.8711677.

[7] P. R. Bhargav, N. L, P. K. Kumar, Compressive sensing based doa estimation for multi-path environment, in: 2021 IEEE International Conference on Mi- crowaves, Antennas, Communications and Electronic Systems (COMCAS), 2021, pp. 309–313. doi:10.1109/COMCAS52219.2021.9629116.

[8] N. L, P. K. Kumar, Performance analysis of sparse array using compressive sensing in a closed multi-path environment, in: 2022 IEEE Microwaves, Antennas, and Propagation Conference (MAPCON), 2022, pp. 1413–1417. doi:10.1109/MAPCON56011.2022.10046420.

[9] Y. C. Eldar, M. Mishali, Robust recovery of signals from a structured union of subspaces, IEEE Transactions on Information Theory 55 (11) (2009) 5302–5316. doi:10.1109/TIT.2009.2030471.

[10] Z. Yang, L. Xie, Enhancing sparsity and resolution via reweighted atomic norm minimization, IEEE Transactions on Signal Processing 64 (4) (2016) 995–1006. doi:10.1109/TSP.2015.2493987.

[11] G. K. Papageorgiou, M. Sellathurai, Y. C. Eldar, Deep networks for direction-of-arrival estimation in low snr, IEEE Transactions on Signal Pro- cessing 69 (2021) 3714–3729. doi:10.1109/TSP.2021.3089927.

[12] M. Q. Nguyen, R. Feger, T. Wagner, A. Stelzer, High angular resolution method based on deep learning for fmcw mimo radar, IEEE Transactions on Microwave Theory and Techniques (2023) 1– 15doi:10.1109/TMTT.2023.3277022.

[13] Y. Kase, T. Nishimura, T. Ohgane, Y. Ogawa, D. Kitayama, Y. Kishiyama, Doa estimation of two targets with deep learning, in: 2018 15th Workshop on Positioning, Navigation and Communications (WPNC), 2018, pp. 1–5. doi:10.1109/WPNC.2018.8555814.

[14] H. Huang, J. Yang, H. Huang, Y. Song, G. Gui, Deep learning for super- resolution channel estimation and doa estimation based massive mimo system, IEEE Transactions on Vehicular Technology 67 (9) (2018) 8549–8560. doi:10.1109/TVT.2018.2851783.

[15] Z.-M. Liu, C. Zhang, P. S. Yu, Direction-of-arrival estimation based on deep neural networks with robustness to array imperfections, IEEE Transactions on Antennas and Propagation 66 (12) (2018) 7315–7327. doi:10.1109/TAP.2018.2874430.

[16] L. Dharma Theja ch, L. Nagaraju, K. Kumar Puli, Classification based doa estimation using ann and cnn models, in: 2022 IEEE Microwaves, An- tennas, and Propagation Conference (MAPCON). doi:10.1109/MAPCON56011.2022.10047297.

[17] E. Ozanich, P. Gerstoft, H. Niu, A deep network for single-snapshot di- rection of arrival estimation, in: 2019 IEEE 29th International Work- shop on Machine Learning for Signal Processing (MLSP), 2019, pp. 1–6. doi:10.1109/MLSP.2019.8918746.

[18] J. Yu, L. Zhang, K. Liu, coherently distributed wideband lfm source localization, IEEE Signal Processing Letters 22 (4) (2015) 504–508. doi:10.1109/LSP.2014.2363843.

[19] J. Y. K. L. Liang Zhang, Cheng-Yu Hung, Linear chirp signal doa estima- tion using sparse time–frequency dictionary, Int J Wireless Inf Networks 27 (2020) 568–574. doi:10.1007/s10776-020-00489-1.

[20] K. Hornik, M. Stinchcombe, H. White, Multilayer feedforward networks are universal approximators, Neural Networks 2 (5) (1989) doi: https://doi.org/10.1016/0893-6080(89)90020-8.

[21] Y. Lecun, L. Bottou, Y. Bengio, P. Haffner, Gradient-based learning applied to document recognition, Proceedings of the IEEE 86 (11) (1998) 2278– 2324. doi:10.1109/5.726791.

*International Journal on Recent and Innovation Trends in Computing and Communication*
*ISSN: 2321-8169 Volume: 11 Issue: 9s*
*DOI: https://doi.org/10.17762/ijritcc.v11i9s.7473*
***Article Received**: 26 May 2023 **Revised:** 20 July 2023 **Accepted:** 05 August 2023*

[22] J. Gu, Z. Wang, J. Kuen, L. Ma, A. Shahroudy, B. Shuai, T. Liu, X. Wang, G. Wang, J. Cai, T. Chen, Recent advances in convolutional neural networks, Pattern Recognition 77 (2018) 354–377. doi: https://doi.org/10.1016/j.patcog.2017.10.013.

[23] M. Wang, Z. Zhang, A. Nehorai, Performance analysis of coarray-based music in the presence of sensor location errors, IEEE Transactions on Signal Processing 66 (12) (2018) 3074–3085. doi:10.1109/TSP.2018.2824283.

[24] M. Jansson, B. Goransson, B. Ottersten, A subspace method for direction of arrival estimation of uncorrelated emitter signals, IEEE Transactions on Signal Processing 47 (4) (1999) 945–956. doi:10.1109/78.752593.

[25] P. Stoica, A. Nehorai, Performance study of conditional and unconditional direction-of-arrival estimation, IEEE Transactions on Acoustics, Speech, and Signal Processing 38 (10) (1990) 1783–1795. doi:10.1109/29.60109.

[26] C. Ozdemiir, Inverse Synthetic Aperture Radar Imaging with MATLAB Algorithms.

## APPENDIX

### *A. Justification of LFM alternate equation*

The LFM signal is typically described using the instantaneous frequency, which is the derivative of the phase with respect to time [26]. In the case of the LFM signal, the phase Φ(t) can be written as:

$$\Phi(t) = \pi(2f_0(t) + \mu_0 t^2) \quad \text{(A.1)}$$

To calculate the instantaneous frequency, we take the derivative of the phase with respect to time:

$$\omega(t) = \frac{d\,\Phi(t)}{dt} = \pi(2f_0 + 2\mu_0 t\,) \quad \text{(A.2)}$$

$$\omega(t) = 2\pi(f_0 + \mu_0 t\,) \quad \text{(A.3)}$$